High energy interactions and the longitudinal behaviour of giant air showers

1974 J. Phys. A: Math. Nucl. Gen. 7 1777

(http://iopscience.iop.org/0301-0015/7/14/010)

J. Phys. A: Math., Nucl. Gen., Vol. 7, No. 14, 1974. Printed in Great Britain.

High energy interactions and the longitudinal behaviour of giant air showers

L Goorevich and L S Peak

Cornell–Sydney University Astronomy Centre, School of Physics, University of Sydney, NSW 2006, Australia

Received 22 January 1974, in final form 16 April 1974

Abstract. A realistic model of nucleon and pion interactions is developed incorporating fast development, possible formation of many pionization centres and production of $N\bar{N}$ pairs.

This model is used to develop air showers with proton primaries via the technique of successive generations.

Comparison of the longitudinal properties of the resulting showers with experimental data at sea level suggests significant nucleon–anti-nucleon production (becoming more dominant for increasing energies) and the need for an even faster development.

1. Introduction

For some time now the Sydney cosmic ray group has been operating an array of muon detectors covering an area of about 60 km^2 in order to detect ultra-high energy extensive air showers.

The number of muons greater than a threshold of 0·75 sec θ GeV is recorded at each station (θ is the zenith angle of the shower). The total number of muons in any particular event (N_μ) is then estimated using a structure function fit; and together with the accurate arrival times at each station, this constitutes the data from which the characteristics of the primary particle are to be inferred.

Perhaps the most important parameter to unfold is the primary energy (E_0) of the shower and (short of a complex array measuring many thresholds at varying radial distances) this conversion must be done by some simulation procedure. Consequently the N_μ–E_0 link is somewhat dependent upon the model used to describe the fundamental interaction processes developing the air shower.

In the past (Goorevich 1971), the Sydney group has used a conversion based upon a conventional two-fireball-isobar type model for nucleon interactions. This has incorporated an $E_0^{1/4}$ multiplicity law and has used a one-dimensional Monte Carlo procedure for shower generation. We now present the results of a substantial revision of this work both in model and simulation technique. Such a revision has become necessary because of:

(i) the inordinately long time involved to generate high energy showers ($E_0 \geqslant 10^{17}$ eV) via the Monte Carlo method.

(ii) The experimentally observed enhanced $N\bar{N}$ production seen at the CERN intersecting storage rings (Albrow *et al* 1972), and as inferred from the Indian experiments (Tonwar and Sreekantan 1971, Sreekantan 1971) investigating charged to neutral ratio and the time structure of hadrons in air showers.

(iii) The experimentally observed ISR angular distribution for proton–proton interactions (Breidenbach *et al* 1972). The experiments suggest a constant centre of mass distribution in rapidity for produced secondaries, which is inconsistent with the idea of only two fireballs receding more and more quickly as the available energy increases.

(iv) The surprisingly quick muon development of air showers. The Sydney recorder, at sea level, sees showers at or *past* maximum development for very large air showers at sea level with energies as high as 10^9–10^{10} GeV. Simulation procedures using constant cross sections need to invoke a fast multiplicity dependence (ie $n_s \propto E_0^{1/4}$ to $n_s \propto E_0^{1/2}$) to predict this correctly.

(v) The observed dependence on energy of cross sections. Until recently it was thought that cross sections had reached an asymptotic value. Now the ISR results (Amendolia *et al* 1973) and cosmic ray data on unaccompanied hadrons (Yodh *et al* 1972) at high altitudes point to a total cross section which rises for a time as $\ln s$ and perhaps as quickly as $\ln^2 s$.

A subsequent paper (in preparation) will investigate the attenuation of giant air showers in their passage through the atmosphere; specifically it will examine the effect of changing cross section, primary particle type and intra-nuclear cascading on such attenuation. This paper aims to develop a realistic model of high energy nuclear collisions using the highest energy data available. Nucleon–anti-nucleon production, rapid development and multi-fireball formation are incorporated naturally into the description.

Using this model, and the technique of successive generations, air showers are simulated for various primary energies and zenith angles. Comparison with experiment allows assignment of optimum values for the parameters used.

An N_μ–E_0 conversion is derived and compared with the results of other simulations. Such a link is of vital importance in the calibration of giant air shower arrays such as the one at Sydney; not only to enable interpretation of features of the primary beam but also to allow intercomparison with other large air shower arrays which detect electrons. The derivation of such an N_μ–E_0 conversion using this up-dated model is the prime aim of this paper.

2. The model

We assume that both pionization and resonant centres are present for π–N and N–N collisions.

2.1. Pionization

This is identical in both pion and nucleon collisions. The pionization energy constitutes 20% of the total centre of mass system (CMS) energy. The mass of each pionization centre is assumed to saturate at a value of 4 GeV/c^2. Thus the number of centres is no longer restricted to two and increases with increasing primary energy. In such a picture, we envisage new centres with low CMS recession being formed continuously as the energy increases. The *overall* CMS angular distribution (the summation of all centres) is assumed to have two different shapes; *firstly* a general two-peaked behaviour in the $\ln \tan \phi/2$ variable (model A) as many emulsion events have been observed in the past with strong two-centre characteristics; and *secondly* a flat rectangular distribution in $\ln \tan \phi/2$ (model B), more in keeping with the recent findings at the CERN ISR (Breidenbach *et al* 1972). Assumptions A and B are about equally successful in predicting

experimental results, though there is a little difference in the resulting N_μ–E_0 conversion. Thus our final conversion becomes a band of possible values between the model limits.

The angular distributions of A and B are both adjusted to give a value of σ (the standard deviation of the laboratory lg tan θ distribution) given by $\sigma = 0{\cdot}38 + 0{\cdot}16 \lg \gamma_c$. This is the result given by the Polish emulsion group (Gierula and Wojnar 1970) summarizing a very careful analysis of simple emulsion interactions up to energies of about 5×10^{13} eV.

Such a situation implies a rather fast multiplicity dependence. Although the multiplicity law is not explicitly injected into the model, the assumed angular distribution and conservation of energy determine uniquely the number of pionization centres. For model A this dependence varies asymptotically as $E_0^{0{\cdot}3}$ at high energies whilst for model B the dependence is more like $E_0^{0{\cdot}35}$.

Each pionization centre decays into about 90% π mesons with mean decay total energy 0·5 GeV and about 10% $N\bar{N}$ pairs with mean decay total energy approximately 1·3 GeV. Anti-nucleons are assumed to be indistinguishable from nucleons.

2.2. Resonant states

If one examines the energy spectra of high energy muons (100–1000 GeV) at sea level, (Abdel-Monem *et al* 1973) and compares them with the primary proton spectrum in the region 10^{12}–10^{13} eV (Ryan *et al* 1972), one sees that the actual integral intensities are not markedly different. If then one assumes that the greatest contribution to the flux of these high energy muons comes from the first interaction in the atmosphere (because of the steepness of the incident energy spectrum), and allowance is made for pion interactions, one is led to the conclusion that in the primary interaction there is a single pion formed which takes away a good fraction of the energy ($\sim$30%).

This conclusion is supported by emulsion study of the angular distributions, interactions and cascade development of the secondaries of interactions. Again one is led to the conclusion that often one or two secondaries take away a large fraction of the available energy.

Consequently it seems natural to assume that in N–N collisions the nucleons can be excited into resonant states which decay strongly to just a few products. Higher mass resonances probably have high spin and their formation would be damped by the centrifugal barrier.

We therefore assume the formation of resonances of mass about 2 GeV/c^2 which decay strongly into a nucleon and a pion. As the isobar component takes 80% of the incident energy, and the backward resonance in the laboratory may be neglected; the isobar nucleon takes a resulting laboratory energy of $0{\cdot}5E_0$ and the isobar pion receives $0{\cdot}3E_0$. This elasticity of 50% seems a most reasonable choice in the light of experiments with accelerators, emulsions and air shower installations.

In the case of π–N collisions, we also assume the formation of resonances. Now, however, we are dealing with boson resonances and a possible decay channel is into an $N\bar{N}$ pair. We assume that the pion resonances (which take 80% of the laboratory energy) decay into an $N\bar{N}$ pair in a fraction χ of the cases, and into three pions (π^+, π^0, π^-) in $(1-\chi)$ of the cases. χ is thus an adjustable parameter which is varied from 0 to 1. It will be seen in later sections that an energy-dependent χ seems to be the best choice, with zero being preferable for low energies and asymptotically approaching one as the interaction energy increases. In our first simple energy-dependent model we have assumed a step transition at an energy of about 10^3 GeV. Table 1 shows some typical

values for models A and B. Typical π–N reactions with $\chi = 1$ are considered for two primary energies, 10^3 and 10^6 GeV.

Table 1. Some typical values of multiplicities and mean energies supplied by models A and B for π–N collisions with $\chi = 1$.

	Model A $\chi = 1$		Model B $\chi = 1$	
E_0 (GeV)	10^3	10^6	10^3	10^6
Number of pionization centres	1·4	24·6	not explicitly calculated	not explicitly calculated
Total number of pions from pionization centres	8·6	15·3	7·7	12·9
Mean energy of pionization pions	18 GeV	1037 GeV	20·8 GeV	1242 GeV
Number of nucleons and anti-nucleons from pionization centres	0·9	15·3	0·8	12·9
Mean energy of pionization nucleons	48 GeV	2710 GeV	52 GeV	3104 GeV
Energy (each) of N and $\bar{\text{N}}$ from resonance decay	$\backsim$400 GeV	$\backsim$400 000 GeV	$\backsim$400 GeV	$\backsim$400 000 GeV

3. Simulation procedure

We set up the analytical diffusion equations for nucleons and pions in the usual fashion. The nucleon and pion mean free paths are taken as 80 and 100 g cm^{-2} respectively. These are written λ_N and λ_π.

The original diffusion equations can be written as follows:

$$\frac{\partial N(E,x)}{\partial x} = -\frac{N(E,x)}{\lambda_N} + \frac{1}{\lambda_N}\int_{E'\geq E} S_{NN}(E,E')N(E',x)\,dE' + \frac{1}{\lambda_\pi}\int_{E'\geq E} S_{\pi N}(E,E')\pi(E',x)\,dE',$$

$$\frac{\partial \pi(E,x)}{\partial x} = -\left(\frac{1}{\lambda_\pi}+\frac{B}{Ex}\right)\pi(E,x) + \frac{1}{\lambda_N}\int_{E'\geq E} S_{N\pi}(E,E')N(E',x)\,dE' + \frac{1}{\lambda_\pi}\int_{E'\geq E} S_{\pi\pi}(E,E')\pi(E',x)\,dE'.$$

$N(E,x)$ and $\pi(E,x)$ are the numbers of nucleons and pions respectively of energy E at a depth of x. x is measured in units of a nucleon mean free path. B is the decay constant for the pions and is set at a value of 139 GeV.

The details of the model enter the calculation via the production spectra. $S_{NN}(E,E')\,dE$ is the number of nucleons in the energy range E to $E+dE$ formed from interactions of nucleons of higher energy E'. Similarly we have $S_{\pi N}(E,E')$, $S_{N\pi}(E,E')$ and $S_{\pi\pi}(E,E')$.

All of these functions need to be considered as there is significant interbreeding of the nucleon and pion cascades.

Specifically we have

$$S_{NN}(E, E') = \delta(E-0{\cdot}5E') + \text{pionization component}$$

$$S_{N\pi}(E, E') = \tfrac{2}{3}\delta(E-0{\cdot}3E') + \text{pionization component}$$

$$S_{\pi N}(E, E') = 2\chi\delta(E-0{\cdot}4E') + \text{pionization component}$$

$$S_{\pi\pi}(E, E') = 2(1-\chi)\delta(E-0{\cdot}27E') + \text{pionization component.}$$

For model A the pionization laboratory energy distribution has the form of a double exponential representing centres moving forward and backward in the CMS

$$P(E)\,dE = c\left[\frac{1}{\gamma_1}\exp\left(-\frac{E}{\gamma_1 kT}\right)+\frac{1}{\gamma_2}\exp\left(-\frac{E}{\gamma_2 kT}\right)\right]dE$$

where γ_1 and γ_2 are the Lorentz factors of the fast and slow centres in the laboratory.

For model B a rectangular rapidity distribution in the CMS leads to an approximately hyperbolic distribution in the laboratory: $P(E)\,dE = K(1/E)\,dE$. The upper and lower bounds are chosen to agree with the Polish data on σ. The procedure then develops the equations in terms of generations in the usual manner. We set

$$N(E, x) = \sum_{l=0}^{\infty}\frac{e^{-x}x^l}{l!}N_l(E)$$

$$\pi(E, x) = \sum_{l=0}^{\infty}\frac{e^{-x}x^l}{l!}\pi_l(E)$$

where $N_l(E)$ is the number of nucleons of energy E contained in the lth generation etc. Substituting and equating coefficients of x^l lead to the following recurrence relations

$$N_l(E) = N_{l-1}(E)\left(1-\frac{1}{\lambda_N}\right)+\frac{1}{\lambda_N}\int_{E'\geq E}S_{NN}(E, E')N_{l-1}(E')\,dE' + \frac{1}{\lambda_\pi}\int_{E'\geq E}S_{\pi N}(E, E')\pi_{l-1}(E')\,dE'$$

$$\pi_l(E) = \left(\frac{lE}{lE+B}\right)\left[\left(1-\frac{1}{\lambda_\pi}\right)\pi_{l-1}(E)+\frac{1}{\lambda_N}\int_{E'\geq E}S_{N\pi}(E, E')N_{l-1}(E')\,dE' + \frac{1}{\lambda_\pi}\int_{E'\geq E}S_{\pi\pi}(E, E')\pi_{l-1}(E')\,dE'\right].$$

Such a procedure enables one to predict the following quantities.

(i) The total number of nucleons and pions as a function of depth and energy.

(ii) The total number of electrons as a function of depth. Given the number of π^0, one can assume immediate decay into two gamma rays of equal energy. One then uses the well known behaviour of soft cascade development (Greisen 1956).

(iii) The total number of muons above any given threshold energy. This calculation incorporates the decay and ionization loss of the muons.

(iv) The behaviour of inclined air showers. This is simply achieved by enhancing the decay constant by a factor sec θ as the zenith angle θ increases.

No mention of lateral distributions will be made in this paper. It has already been shown (Goorevich and Peak 1973) that this calculation gives reasonable agreement with observed muon lateral distributions up to 100 GeV/c for a reasonable average transverse momentum of 0·5–1·0 GeV/c, indicating that the energy distribution of the produced pions is not wildly wrong. However for the detailed examination of the longitudinal properties of air showers, which follows in the next section, no such lateral parameter is needed; and the extra assumptions of the optimum value, the shape of the P_T distribution and the energy dependence for the various particles, are avoided.

We thus have a choice between models A and B with values of χ ranging between 0 and 1. Various tests have been applied to this simulation procedure.

(i) Conservation of energy. It is found that energy is conserved to an accuracy of about 98% from generation to generation.

(ii) A detailed examination of the print-out of the first generation., Hence all quantities, such as limits to the energy distributions, and multiplicity can be calculated and compared with the computer output.

(iii) The pion and nucleon cascade development. By setting $\chi = 0$ and allowing no $N\overline{N}$ pairs from the pionization centres, one can effectively isolate the two cascades—as now no nucleons can come from pion interactions. Thus the behaviour of the nucleon cascade can be examined in its passage through the atmosphere. In particular, there should be only one leading baryon in the entire air shower.

4. Comparison with experiment

4.1. Electron development

We begin by examining the differences between models A and B with $\chi = 0$ and $\chi = 1$. Table 2 summarizes the pertinent results.

Table 2. Electron characteristics for differing models and primary energies.

	E_0 (GeV)	Depth of maximum development (g cm^{-2})	N_e at maximum development	Mean energy per particle (GeV)
Model A $\chi = 0$	10^7	∽720	$4{\cdot}78 \times 10^6$	2·1
	10^8	∽800	$4{\cdot}77 \times 10^7$	2·1
	10^9	∽880	$4{\cdot}58 \times 10^8$	2·2
Model A $\chi = 1$	10^7	∽720	$3{\cdot}8 \times 10^6$	2·6
	10^8	∽800	$3{\cdot}86 \times 10^7$	2·6
	10^9	∽880	$3{\cdot}66 \times 10^8$	2·7
Model B $\chi = 1$	10^7	∽720	$5{\cdot}48 \times 10^6$	1·8
	10^8	∽800	$5{\cdot}52 \times 10^7$	1·8
	10^9	∽840	$5{\cdot}19 \times 10^8$	1·9

It is seen that all models predict maxima at approximately the same depth for a given primary energy, and that the mean energy per particle at maximum development in all cases is close to the generally accepted figure of 2 GeV per particle. As the multiplicities and energy distributions of the pionization products are not very different for

models A and B (see for example table 1); and as the parameter χ has no effect on the pionization secondaries which constitute the bulk of the products, it is perhaps to be expected that the position of maximum development is model independent.

The Chacaltaya results (La Pointe *et al* 1968) show development curves with maxima which are higher in the atmosphere. For a 10^8 GeV primary, for example, the experimental maximum is around 650 g cm^{-2} whilst the simulated value is close to 800 g cm^{-2} giving a discrepancy of about 150 g cm^{-2}.

For a primary with $A = 50$, a 10^8 shower would be (to a first approximation) a superposition of showers of energy about 2×10^6 GeV. The simulation puts maxima for this energy at about 680 g cm^{-2}. As the first interaction is itself higher in the atmosphere, the effect of heavy primaries can go a long way towards removing this discrepancy.

Figure 1 shows some typical development curves for vertical primary protons.

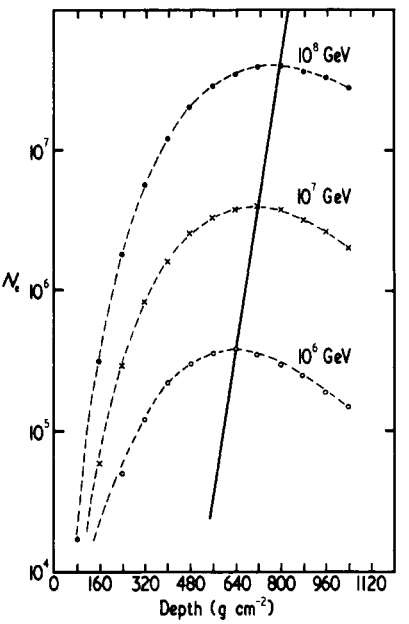

Figure 1. Simulated electron development curves for vertical primary protons of various primary energy E_0.

4.2. N_μ–N_e dependence

Figure 2 shows the predicted sea level N_μ–N_e dependence for models A ($\chi = 0$, $\chi = 1$) and B ($\chi = 1$). Although the absolute values are slightly different, the lines are closely parallel with a slope of about 0·83–0·86.

The Sydney spark chamber experiment, operating in conjunction with the giant muon array has examined structure functions closely, and has come up with an experimental dependence $N_\mu \propto N_e^{0.85 \pm 0.07}$ for sea level values (Bell *et al* 1973). Also shown in figure 2 are the experimental results, for the same threshold, of the Tokyo group (Fukui *et al* 1960, Hasegawa *et al* 1963). It can be seen that the actual simulation values are of the correct magnitude though the resolution is not sufficient to favour one model against the other. This is particularly so for the high energy experimental point ($N_e = 10^7$) where the data are very sparse.

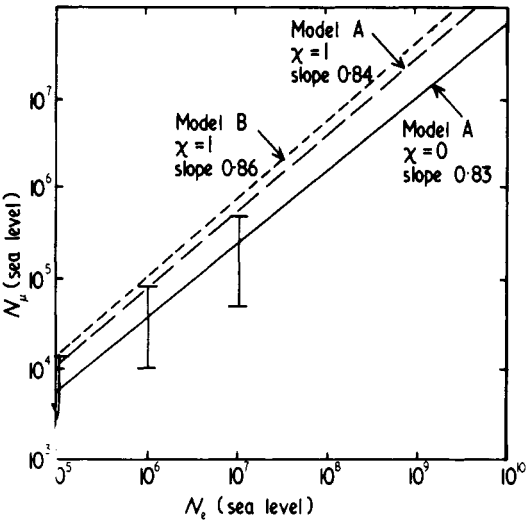

Figure 2. The N_μ–N_e dependence at sea level for various models. The muon threshold is 1 GeV. Also plotted are the experimental results of the Tokyo group; the bounds plotted are the observed spread in N_μ for three fixed values of N_e.

4.3. Hadron spectra

Figures 3(*a*) and (*b*) show the number of hadrons with energy above 100 GeV and 1000 GeV respectively as a function of sea level shower size. The predictions are for model A with $\chi = 0$ and $\chi = 1$. The results of model B are virtually identical. Also plotted are the results from (Kameda *et al* 1965) who used a multi-plate cloud chamber in conjunction with an extensive air shower array. Another experiment (Fritze *et al* 1970) using a neon hodoscope and examining hadrons greater than 800 GeV finds good agreement with the Kameda *et al* results. The slope of the simulated lines is close to

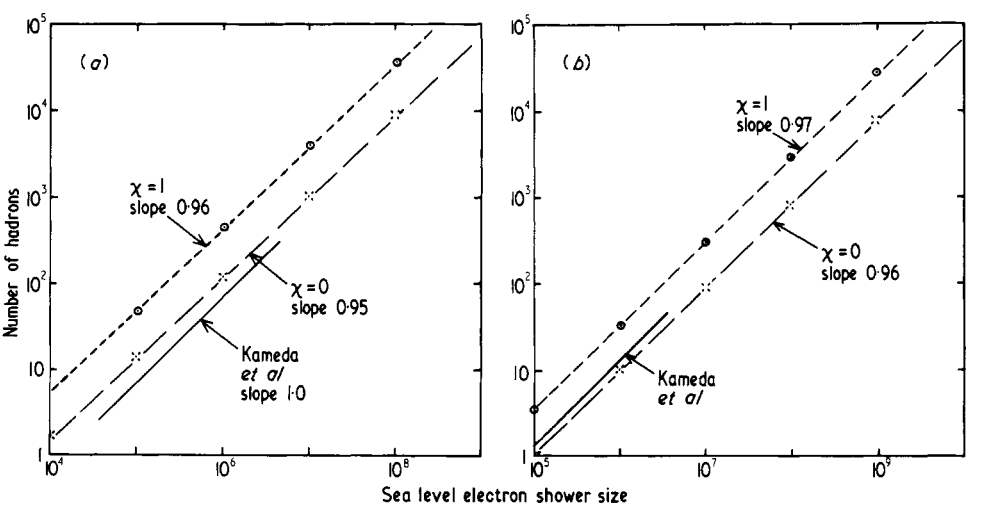

Figure 3. The number of hadrons with energy greater than (*a*) 100 GeV and (*b*) 1000 GeV as a function of sea level electron shower size. The simulated lines are for model A with $\chi = 0$ and $\chi = 1$. The predictions for model B are similar. The full line represents the results of Kameda *et al*.

about 1·0, showing that the number of hadrons greater than any fixed threshold rises nearly linearly with shower size. This result is seen by Kameda *et al.*

When comparing absolute numbers extreme caution must be exercised. The Sydney group has operated an array of plastic scintillators (Winn *et al* 1965) in order to examine the core structure of extensive air showers. Two rather distinct classes of event emerged from this investigation—the first,were the single-cored events which have a single defined core region, the second class of events could be called flat-top showers with no such sharp core and often displaying two or more sub-cores. The first of these types is attributable to showers caused by incident proton primaries whilst the second could well be caused by primaries other than protons.

The Sydney experiment has revealed marked differences in the hadron content of the two types of shower. This is demonstrated in table 3 which shows the mean number of hadrons detected with energy greater than 160 and 1600 GeV as a function of shower size. These results were obtained when half of the scintillators were shielded by 30 cm of lead to investigate hadron content and half were left unshielded to discern the core type involved.

Table 3. The observed number of hadrons greater than 160 and 1600 GeV hitting the Sydney scintillator array; as a function of shower size for single-cored and flat-topped showers.

	Number of hadrons with $E > 160$ GeV		Number of hadrons with $E > 1600$ GeV	
Shower size	Single core	Flat top	Single core	Flat top
$10^5 \leqslant N < 3\times10^5$	2·6 ± 0·3	0·9 ± 0·1	0·5 ± 0·2	0
$3\times10^5 \leqslant N < 7\times10^5$	4·1 ± 0·5	1·4 ± 0·15	0·5 ± 0·2	0
$7\times10^5 \leqslant N < 10^6$	10·2 ± 1·4	2·0 ± 0·4	1·8 ± 0·6	0
$10^6 \leqslant N < 5\times10^6$	17·5 ± 3·0	5·7 ± 0·5	2·5 ± 1·1	0·3 ± 0·1

Thus any experiment which does not differentiate between these classes of core behaviour will presumably trigger on a mixture and thus would measure a lower number of hadrons than a pure proton sample. (The amount of this mixture depends upon the triggering criterion of the particular experiment in question.)

This is probably the reason for the discrepancy between the proton simulation results and the experimental data.

Figure 4 shows the integral energy spectrum of hadrons normalized to a shower size of 2×10^6. The Kameda results are again shown together with the results of Matano *et al* (1970) extending up to thresholds of about 10 TeV. From the figure we can make the following observations.

(i) The spectra of Kameda *et al* and Matano *et al* agree rather well—one being a natural extension of the other. (Kameda predicted a steepening for higher hadron energies.)

(ii) The simulation values are greater than the observed number of hadrons for small hadron energy—an effect perhaps to be expected from the above discussion.

(iii) The energy dependent curve gives the better reproduction of the shape of the spectrum and asymptotically approaches the $\chi = 1$ curve for high thresholds.

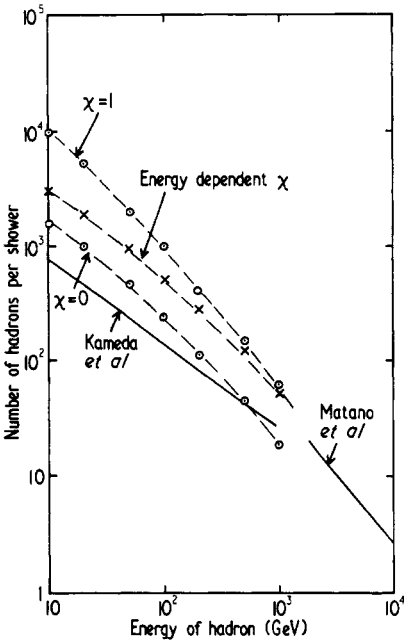

Figure 4. The integral energy spectrum of hadrons at sea level normalized to electron shower size of 2×10^6. The broken lines are simulation results for model A, $\chi = 0$, $\chi = 1$, and an energy dependent χ with transition energy 1000 GeV ($\chi_{1000}(E)$). The full lines represent the experimental results of Kameda *et al* (1965) and Matano *et al* (1970).

(iv) The extrapolation of the $\chi = 0$ curve would be far too low to explain the experimental observations at high energies—whereas the $\chi = 1$ and $\chi_{1000}(E)$ curves fit naturally onto the Matano results. This would be expected if the experimental data had a triggering bias towards proton showers for high hadron thresholds.

Thus at high thresholds, simulations involving resonant production of nucleon-anti nucleon pairs give the better agreement with experiment.

4.4. Charged to neutral ratio

The suggestion that an energy dependent χ is needed, is further strengthened by examination of the charged to neutral ratio for hadrons in air showers. Kameda *et al* find the following values (which are roughly independent of shower size).

Threshold energy (GeV)	Charged to neutral ratio R
100–500	6 ± 1
500–1000	$2{\cdot}5^{+1{\cdot}5}_{-0{\cdot}5}$
> 1000	$1{\cdot}5 \pm 0{\cdot}5$

The Indian experiment at 800 g cm^{-2} (Vatcha *et al* 1972, Vatcha and Sreekantan 1972) presents a similar result; with the ratio being independent of shower size for high thresholds and approaching one as the threshold increases. Model A gives values for R

around 10–12 for $\chi = 0$, whilst $\chi = 1$ gives values about 1·9. These values are fairly independent of shower size and threshold. If we try an energy dependent χ with transition energy around 10^3 the results give reasonable agreement with experiment as is seen in table 4.

Table 4. Behaviour of charged to neutral ratio of hadrons as a function of the primary energy and the threshold energy, for four different assumed dependences of χ.

Threshold (GeV)	R ($E_0 = 10^7$ GeV)	R ($E_0 = 10^8$ GeV)	
100	1·9	1·91	Transition energy 0 ie $\chi = 1$
500	1·9	1·93	
1000	1·8	1·95	
100	3·0	3·0	Transition energy 10^3 GeV
500	1·86	1·93	
1000	1·81	1·94	
100	5·24	5·4	Transition energy 5×10^3 GeV
500	2·94	3·26	
1000	2·10	2·41	
100	10·14	11·30	Transition energy ∞ ie $\chi = 0$
500	10·41	10·78	
1000	12·2	9·99	

4.5. Muon spectra

The integral energy spectra of muons at sea level have been calculated for models A and B.

Figure 5 shows the results of model B for two shower sizes (the results of model A are virtually identical). Also shown are the muon spectrograph measurements of Earnshaw *et al* (1967) valid for muons of energy 100 GeV or less and shower sizes between 10^5 and 10^8 particles. It can be seen that the energy dependent χ with a transition energy of 1000 GeV ($\chi_{1000}(E)$) gives the best reproduction of the shape and absolute values. The absolute values predicted by $\chi = 0$ are too low for low muon energies whilst the slope of the $\chi = 1$ curve is too steep in the same region.

4.6. Muon attenuation

The Sydney experimental array measures the attenuation of showers by examining the integral spectra for different zenith angles. A constant integral intensity cut represents a type of development curve, remembering, of course, that the threshold energy of muons increases with increasing zenith angle. The Sydney threshold is close to 0·75 sec θ GeV.

Using this technique, the experimental curves show that all but the largest showers are past maximum muon development at sea level. The largest showers observed by the Sydney array (with vertical muon size $\gtrsim 10^8$) appear to be very roughly at maximum development at sea level. The experimental curves are reasonably approximated by a straight line on a $\ln(N_\mu)$ linear ($\sec\theta$) graph; and consequently it is meaningful to define a parameter λ such that

$$N_\mu(\theta) = N_\mu(0) \exp\left(\frac{1 - \sec\theta}{\lambda}\right).$$

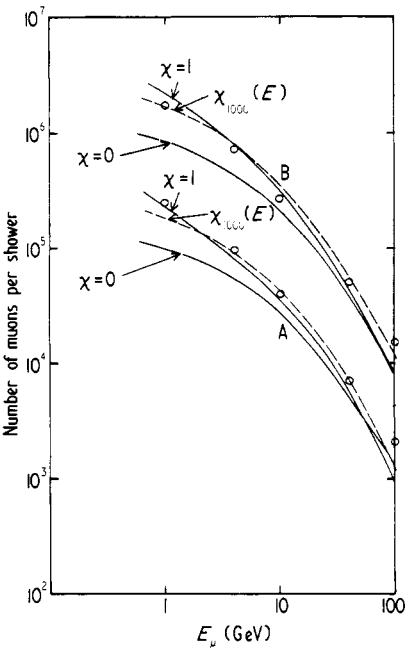

Figure 5. The integral energy spectrum of muons at sea level for model B with an energy dependent χ (transition energy 1000 GeV), $\chi = 0$ and $\chi = 1$ for electron shower sizes of $3{\cdot}1 \times 10^6$ (A) and 4×10^7 (B). The experimental points (○) are from Earnshaw *et al* (1967).

The simulation program also gives the value of λ calculated in a similar way with account taken of the variation of threshold energy. The resulting curves are also well represented by the exponential dependence above, and the results for λ are summarized in table 5. As in the experimental case, the development for all but the largest showers is

Table 5. Attenuation parameter, λ, of simulated showers for differing models and primary energies.

E_0 (GeV)	Model A		Model B
	$\chi = 0$	$\chi = 1$	$\chi = 1$
10^7	1·2	1·0	1·01
10^8	1·25	1·06	1·08
10^9	1·3	1·13	1·16

past maximum, with showers of $E_0 \sim 10^{10}$ GeV being at approximately maximum muon development at sea level. It is seen that there is virtually no difference in the attenuation predicted by models A and B. In all cases the development of the shower is somewhat slower than seen experimentally—a result also noted by Hillas using a wide variety of models. Figure 6 shows the attenuation data for the Sydney muon array. It can be seen that the experimental errors are rather large resulting in a wide range for λ. For example the extreme slopes for the experimental points with N_μ (vertical) $= 10^7$ is

$$0{\cdot}57 \leqslant \lambda \leqslant 1{\cdot}66.$$

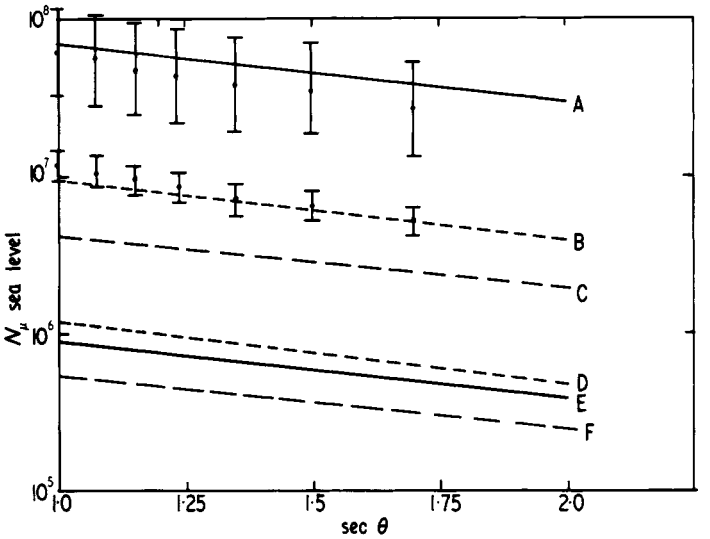

Figure 6. Attenuation data of the Sydney giant muon array, SUGAR, compared with various simulations from the text and with Hillas models A and J. λ is defined by

$$N_\mu(\theta) = N_\mu(0)\exp\left(\frac{1-\sec\theta}{\lambda}\right)$$

where the muon threshold for any angle is $0{\cdot}75\sec\theta$ GeV. Curve A, $E_0 = 10^{10}$ GeV, Hillas models A and J, $\lambda = 1{\cdot}2$; curve B, $E_0 = 10^9$ GeV, $\chi = 1$, $\lambda = 1{\cdot}13$; curve C, $E_0 = 10^9$ GeV, $\chi = 0$, $\lambda = 1{\cdot}3$; curve D, $E_0 = 10^8$ GeV, $\chi = 1$, $\lambda = 1{\cdot}06$; curve E, $E_0 = 10^8$ GeV, Hillas model A, $\lambda = 1{\cdot}2$; curve F, $E_0 = 10^8$ GeV, $\chi = 0$, $\lambda = 1{\cdot}25$.

The curves for $\chi = 0$ and $\chi = 1$ are plotted for two primary energies 10^8 and 10^9 GeV. The slopes for $\chi = 1$ are closer to the SUGAR data than those for $\chi = 0$. Though not completely reproducing the steep experimental slope the agreement is marginally better than the values for Hillas models A and J (also plotted).

The best estimate for the SUGAR value of λ can be quoted as

$$\lambda = 0{\cdot}78 + 0{\cdot}14\lg\left(\frac{N_\mu(0)}{10^7}\right) \quad \text{atm.}$$

It should be noted that the absolute values of N_μ quoted in figure 6 are not relevant—as the experimental points are cuts for a given integral intensity whilst the theoretical values are for fixed primary energy. The integral intensities have been chosen so that the values of the muon data would be roughly comparable with the simulation values—however detailed comparison between the two is not possible.

In conclusion we can state that although the attenuation observed by the Sydney array can be reproduced within the error bars by the present simulation the mean attenuation seems to be somewhat faster than can be predicted by this simulation or any other conventional treatment. As both models A and B have a fast multiplicity dependence upon primary energy, the fast experimental development seen is probably caused by the additional effect of heavy primaries, changing cross section with energy and intra-nuclear cascading. Of these added effects, preliminary investigation shows

that simply changing to heavy primaries is insufficient to fully reproduce the exper mental situation.

The effect of changing cross section, heavy primaries and intra-nuclear cascading in the context of this up-to-date model, will be discussed at length in a subsequent paper.

4.7. N_μ–E_0 conversion

Figure 7 shows the resulting sea level conversion for N_μ–E_0 for vertical showers and a muon threshold energy of 0·75 GeV. Models A and B are plotted; the extreme cases are model A $\chi = 0$ (lower bound) and model B $\chi = 1$ (upper bound). These then define the region of uncertainty resulting from the foregoing treatment. The results using an energy dependent χ naturally lie within these bounds and the case for model A with a transition energy of 1000 GeV is plotted.

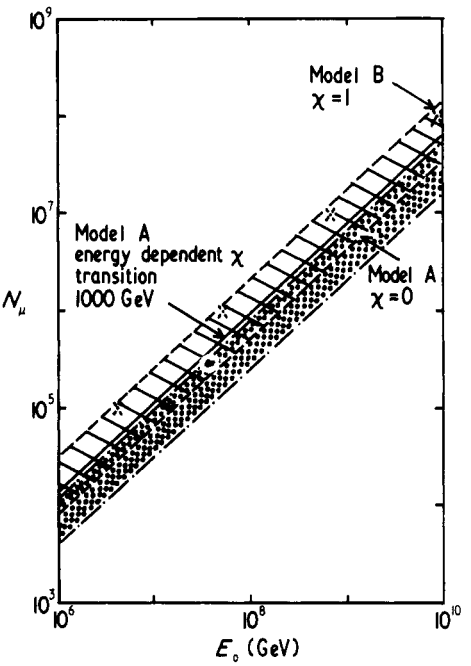

Figure 7. The N_μ–E_0 conversion at sea level for muons with threshold 0·75 GeV. The conversion is for vertical showers of proton primaries. The dotted region represents the area covered by most conventional simulations. The individual points (×) represent the former Sydney conversion. The shaded region summarizes the bounds of the present treatment.

Also shown is the old Sydney conversion using a Monte Carlo technique and invoking an $E_0^{1/4}$ multiplicity (Goorevich 1971). This treatment has since been discarded because of its rather unsatisfactory zenith angle behaviour, but for vertical showers the conversion lies within the newly defined region.

The region covered by most other conventional simulations is also shown—all of these conversions assume a proton primary.

5. Conclusion

We have constructed a reasonably realistic model of nuclear collisions incorporating the latest results from accelerators and air shower installations. These results include enhanced $N\bar{N}$ production, fast multiplicity increase and possible formation of many pionization centres at high energies.

Restricting our consideration to proton primaries with constant cross section we find that best agreement is achieved with experimental data by invoking an energy-dependent production of nucleon–anti-nucleon pairs starting to become dominant somewhere between 10^{12} and 10^{13} eV.

Using this model we find good agreement with muon and hadron spectra both in shape and absolute numbers per shower. The charged to neutral ratio and electron development are also well duplicated as is the N_μ–N_e connection at sea level. Examination of the development of showers suggests that showers are reaching maximum and dying away surprisingly quickly. To exactly reproduce the observed development of giant air showers some other factor causing fast development (such as an energy dependent cross section) is needed.

Acknowledgments

We are indebted to Professor H Messel for the provision of such excellent facilities and to Professor C B A McCusker for constant advice and encouragement. We have been supported financially by the Science Foundation for Physics within the University of Sydney, the Australian Research Grants Committee and the US Air Force Office of Scientific Research.

Appendix

Table 6. Some of the typical values for simulations of vertical showers with $\chi = 0$ and 1 and $E_0 = 10^5$, 10^7 and 10^9 GeV. The values have been computed using model A.

	$\chi = 0$			$\chi = 1$		
E_0 (GeV)	10^5	10^7	10^9	10^5	10^7	10^9
N_e max	$5{\cdot}2 \times 10^4$	$4{\cdot}8 \times 10^6$	$4{\cdot}6 \times 10^8$	$4{\cdot}0 \times 10^4$	$3{\cdot}8 \times 10^6$	$3{\cdot}7 \times 10^8$
t_{max} (g cm^{-2})	~560	~720	~880	~560	~720	~880
N_e sea level	$1{\cdot}09 \times 10^4$	$2{\cdot}39 \times 10^6$	$3{\cdot}82 \times 10^8$	$1{\cdot}03 \times 10^4$	$2{\cdot}06 \times 10^6$	$3{\cdot}10 \times 10^8$
$N_\mu(>1$ GeV) sea level	$1{\cdot}09 \times 10^3$	$6{\cdot}28 \times 10^4$	$3{\cdot}75 \times 10^6$	$1{\cdot}82 \times 10^3$	$1{\cdot}26 \times 10^5$	$8{\cdot}2 \times 10^6$
$N_\mu(>100$ GeV) sea level	$2{\cdot}21 \times 10$	$6{\cdot}96 \times 10^2$	$3{\cdot}51 \times 10^4$	$1{\cdot}63 \times 10$	$5{\cdot}57 \times 10^2$	$3{\cdot}5 \times 10^4$
$N_{hadrons} > 100$ GeV	1·78	$2{\cdot}94 \times 10^2$	$2{\cdot}8 \times 10^4$	4·3	$9{\cdot}94 \times 10^2$	$1{\cdot}03 \times 10^5$
$N_{hadrons} > 1000$ GeV	0·11	22·5	$3{\cdot}0 \times 10^3$	0·15	63	$9{\cdot}51 \times 10^3$

References

Abdel-Monem M S, Benbrook J R, Duller N M, Green P J, Osborne A R and Sheldon W R 1973 *Proc. 13th Int. Conf. on Cosmic Rays, Denver* vol 3 (Denver: University of Denver) pp 1811–5

Albrow *et al* 1972 *Phys. Lett.* **40B** 136–40

Amendolia S R *et al* (Pisa–Stony Brook collaboration) 1973 *Phys. Lett.* **44B** 119–24

Bell C J *et al* 1973 *Proc. 13th Int. Conf. on Cosmic Rays, Denver* vol 4 (Denver: University of Denver) pp 2569–74

Breidenbach *et al* 1972 *Phys. Lett.* **39B** 650–4

Earnshaw J *et al* 1967 *Proc. Phys. Soc.* **90** 91–108

Fukui S *et al* 1960 *Prog. Theor. Phys., Suppl.* **16** 1–53

Fritze *et al* 1970 *Acta Phys. Acad. Sci. Hung.* **29** *Suppl.* 3 439–45

Gierula J and Wojnar E 1970 *Acta Phys. Acad. Sci. Hung.* **29** *Suppl.* 3 119–23

Goorevich L 1971 *Proc. 12th Int. Conf. on Cosmic Rays, Hobart* vol 3 (Hobart: University of Tasmania) pp 983–8

Goorevich L and Peak L S 1973 *Proc. 13th Int. Conf. on Cosmic Rays, Denver* vol 4 (Denver: University of Denver) pp 2617–24

Greisen K 1956 *Progress in Cosmic Ray Physics* vol 3 (Amsterdam: North Holland) p 1

Hasegawa *et al* 1963 *J. Phys. Soc. Japan* **17** *Suppl.* A-III 189–95

Kameda *et al* 1965 *Proc. 9th Int. Conf. on Cosmic Rays, London* (London: The Institute of Physics and the Physical Society) pp 681–4

La Pointe M *et al* 1968 *Can. J. Phys.* **46** 68–71

Matano T. Machida M and Ohta K 1970 *Acta Phys. Acad. Sci. Hung.* **29** *Suppl.* 3 451–62

Ryan M J *et al* 1972 *Phys. Rev. Lett.* **28** 985–8

Tonwar S C and Sreekantan B V 1971 *J. Phys.* A: *Gen. Phys.* **4** 868–82

Sreekantan B V 1971 *Proc. 12th Int. Conf. on Cosmic Rays, Hobart* vol 7 (Hobart: University of Tasmania) pp 2706–19

Vatcha R H and Sreekantan B V 1972 *Tata Institute of Fundamental Research Preprint* No CR-EAS-9

Vatcha R H, Sreekantan B V and Tonwar S C 1972 *J. Phys.* A: *Gen. Phys.* **5** 859–76

Winn M M *et al* 1965 *Nuovo Cim.* **36** 701–32

Yodh G B. Yash Pal and Trefil J S 1972 *Phys. Rev. Lett.* **28** 1005